PHYSICAL REVIEW D VOLUME 50, NUMBER 9 1 NOVEMBER 1994

Solving Schrödinger's equation for pure SU(3) on a large lattice

J. B. Bronzan* and Yüksel Günal
Department of Physics and Astronomy, Rutgers University, Piscataway, New Jersey 08855-0849
(Received 26 May 1994)

We study the solution of Schrödinger's equation for pure SU(3) lattice gauge theory on a $10\times10\times10$ spatial lattice. Our basis consists of 9001 states of modified Krylov-type. No gauge fixing is used. Instead we work on an ensemble of basis states each having different color content on the lattice. Physical (colorless) results are obtained by extrapolation in color. We determine the physical ground state energy density from strong to weak coupling at the 10% level of accuracy. We show that physical glueball masses can be measured by our method. Our basis must be improved to see scaling and obtain continuum results.
PACS number(s): 11.15.Ha, 12.38.Gc, 12.38.Lg

I. INTRODUCTION

It is customary to study lattice gauge theory numerically by the approximate evaluation of Feynman's path integral. By contrast, in this paper we consider the construction of approximate solutions of Schrödinger's equation. We believe this is worthwhile because the approaches differ in useful ways. For example, the path integral easily explores the theory at high temperature, while Schrödinger's equation is well suited to the case of zero temperature. Monte Carlo algorithms have the advantage of converging (slowly) to exact results. On the other hand, when Schrödinger's equation is solved, one can implement hunches through the choice of states included in the basis set, or perhaps through variational parameters. See [1] for a discussion of further contrasts between the approaches.

Many obstacles must be overcome to solve Schrödinger's equation, as the literature attests [1, 2]. In this paper we examine the subject and set up a computer program to generate approximate solutions of Schrödinger's equation. As we go along, we shall make choices and propose solutions to the obstacles we meet. Because we have QCD in mind, the theory we study is pure SU(3) lattice gauge theory in three spatial dimensions. This theory omits fermions, but it retains the complication of gauge wave functions built on the SU(3) manifold. It also poses the central problem in solving Schrödinger's equation: coping with a huge number of degrees of freedom (DF). The lattice we work with is $10 \times 10 \times 10$, not large by Monte Carlo standards. However, the lattice has 3000 link DF on it, which is enough to force us to devise a general method for the large number of DF. In our approach the addition of fermions is probably not a major obstacle [6].

This paper follows a series of previous papers that have dealt with a number of issues that arise in solving Schrödinger's equation for SU(3) lattice gauge theory. One of these papers concerns the constuction of "harmonic oscillator" states on SU(3) [3]. These harmonic oscillator states are single DF states that are well suited to our problem. Included in that paper is the evaluation of matrix elements of the single DF operators that appear in the SU(3) Hamiltonian. A second paper applies harmonic oscillator states to construct approximate solutions of SU(3) on a tiny lattice (a cube) [4]. Other work extends the results by considering more elaborate bases for the cube [5], and by adding Kogut-Susskind fermions to the cube (making a prototype of QCD) [6].

We must use a finite basis for our computer work, which is a requirement that is difficult to reconcile with the large number of DF in the problem. We cannot provide each DF with its own basis of K states, because that leads to a basis of K^{3000} states on our lattice, which is intractable for any $K > 1$. In addition, the basis we use must meet physically motivated requirements. First, the basis must provide for long-range correlations because continuum results are obtained by tuning the theory to the regime of long correlation length and then matching to renormalization group expressions. In addition, the basis must provide for corrections that can tile the whole lattice if changes to the ground state energy *density* are to be encompassed. We use a basis of states on the Krylov subspace obtained by applying an effective Hamiltonian repeatedly to a suitable "starting state" $|0\rangle$: $\psi_K = \bar{H}^K|0\rangle$. In Sec. II we discuss the variational origin of this choice, how it meets the requirements mentioned, and why we might expect the results to converge.

In Sec. III we consider the Hamiltonian. The Kogut-Susskind Hamiltonian [7] is invariant under local gauge transformations. Either the unwanted gauge DF must be removed [8, 9], or care must be taken to ensure that basis states are gauge invariant ("colorless") [2], or a procedure must be developed to extrapolate "colored" results to "color"=0. In fact, both gauge fixing the Hamiltonian, and maintaining strict gauge invariance of the basis states lead to an algebraic bog. Therefore, we will use extrapolation to color=0 to obtain results in the physical sector of the theory.

In Sec. IV we discuss the choice of the "starting state" $|0\rangle$, using known properties of the SU(3) ground state at

*Electronic address: bronzan@physics.rutgers.edu

weak and strong coupling as a guide. We introduce an appropriate state on SU(3) which is easy to work with and can be tuned to have the desired properties at both $g = 0$ and $g = \infty$. (The physically relevant scaling region lies *between* these limits.)

In Sec. V we examine the structure of the states $\bar{H}^K|0\rangle$. They are shown to be sums of terms, each of which is a superposition of a number of clusters of excitation. We compress the description of these lattice states by storing the clusters and then using a standard algorithm to write the lattice basis states in terms of clusters when they are needed.

Next, we must construct matrix elements of the SU(3) Hamiltonian between lattice basis states. Because our basis states are so complicated, a naive estimate suggests that these matrix elements are computationally intractable. However, combinatorial factors present in the cluster expansion are closely related to factors in the multinomial expansion, which permits us to write generating functions for matrix elements. These generating functions can be manipulated to put matrix elements in a form that is easily computable in terms of cluster amplitudes. These matters are explained in Sec. VI.

In the end, we must compute the low-lying states of an (approximately) 9000×9000 sparse Hermitian Hamiltonian matrix. This task is practically the least of our problems. Numerical results are presented in Sec. VII.

II. GENERATING BASES

Consider a quantum mechanical system having Hamiltonian H and pick some normalized state $|0\rangle$. The Rayleigh-Ritz principle states that $\langle 0|H|0\rangle$ is an upper bound to the ground state energy. This bound will be strengthened by adding another state to the basis, but in a typical problem involving many DF, it is far from obvious what second state to choose. One way to make a "dynamical" choice (and evade thinking) is to use a state related to $|0\rangle$, say $\hat{O}|0\rangle$. A simple variational calculation shows that (in the absence of further information) the optimal choice is $\hat{O} = H$. Repeating this procedure, we are led to the Krylov basis $\psi_K = H^K|0\rangle$, $K = 1, \ldots, P$. With P finite, it can be shown the ordered eigenvalues of the $P \times P$ Hamiltonian matrix are upper bounds to the lowest P eigenvalues of H [10].

The basis obtained in this way meets the criteria mentioned in the Introduction. Later we will choose $|0\rangle$ to be separable, so the starting state has no correlations at all between different DF. However, the Hamiltonian for SU(3) has terms that act on links separated by one lattice spacing, so when K is of order the *length* of the lattice (10 in our case), there will be terms in ψ_K in which *one* pair of DF across the lattice from each other are correlated. For larger K, there will be *many* such correlated DF, and hence a nonzero correlation length. Similarly, the Hamiltonian for SU(3) has terms that act on either one or four DF, so when K is of order the *volume* of the lattice (1000 in our case) there will be terms in ψ_K in which every DF has been "excited." This opens the possibility of a correction to the energy density (or an *extensive* shift in the energy). If we want to fill the lattice with correlated excitation pairs at arbitrary locations, we need about $10^6 = 1000 \times 1000$ states in the basis.

But why should a moderate-sized Krylov basis give reliable eigenvectors? When the Krylov basis states ψ_K are reorganized as an othonormal set $\{\phi_k\}$, the action of H is of "tridiagonal" form:

$$H\phi_K = d_K\phi_K + e_K\phi_{K+1} + e^*_{K-1}\phi_{K-1}. \tag{2.1}$$

Suppose that we form a matrix of the first P of these states, and that the lowest eigenvalue of this matrix is E_0 with the eigenvector

$$\phi = \sum_{n=0}^{P} a_n\phi_n. \tag{2.2}$$

Then, on the full Hilbert space we have

$$|H\phi - E_0\phi| = |e_P a_P|. \tag{2.3}$$

Under favorable circumstances, we might expect $|a_P| = O(P^{-1/2})$, and $e_P = O(P^0)$. Under these circumstances, the error in the eigenvector is controlled by the size of the basis, not the size of the lattice, and by the usual variational argument, the error in E_0 is $O(P^{-1})$.

The states ψ_K rapidly become complicated, and it is unclear that all the complexity is required for the states to do a good job in lowering energy bounds. To make our basis manageable we construct only approximate renditions of $H^K|0\rangle$. One of the main approximations we will use is to evaluate these states on a subspace. That is, when we insert complete sets of states,

$$\psi_K = \sum_{\{s_i\}} |s_K\rangle\langle s_K|H|s_{K-1}\rangle \cdots \langle s_1|H|0\rangle, \tag{2.4}$$

we will truncate the sums over states. This procedure limits the types of excitations allowed, but it does not limit the correlation length or number of excitations.

In Sec. III we will encounter the case where there is a Hermitian (positive) operator Q^2, a color operator, that commutes with H. Energy eigenstates are also eigenstates of Q^2, and now the problem becomes the determination of energy eigenstates belonging to specific eigenvalues of Q^2. (Our interest will be focused on physical states having eigenvalue zero.) It is difficult to compute simultaneous eigenstates exactly, but it is easy to reconsider the problem of minimizing the energy, now subject to the additional constraint $\langle Q^2\rangle = q^2$. As we shall see, this construction will ultimately lead to results at the physical limit $\langle Q^2\rangle = 0$.

We therefore reconsider the added state $\hat{O}|0\rangle$. When the constraint $\langle Q^2\rangle = q^2$ is added to the energy functional by Lagrange multiplier, the variational choice for $\hat{O}$ is

$$\hat{O} = \frac{\epsilon H + \zeta Q^2 + \eta}{\alpha H + \beta Q^2 + \gamma}, \tag{2.5}$$

where $\alpha, \ldots$ are constants that we do not further specify. This is not a very convenient operator, but a substitute is

$$\bar{H} = H + \lambda Q^2. \tag{2.6}$$

The basis $\psi_K = \tilde{H}^K|0\rangle$ can be used to make a power series approximation to $\hat{O}$, Eq. (2.5).

Our bases are parametrized by λ, and the Kth-ordered eigenvalue E_K of the $P \times P$ Hamiltonian matrix will depend upon λ. Later we will introduce a second parameter t. The expectation q^2 in the Kth level will also depend upon λ and t. By studying an *ensemble* of bases for different choices of λ, and t, we can determine the best upper bounds (within the ensemble) to the Kth energy. This bound varies with q^2: $E_K(q^2)$. We discuss how this information will be used in the next section.

III. THE HAMILTONIAN AND COLORED STATES

The Kogut-Susskind Hamiltonian [7] for SU(3) lattice gauge theory is

$$H = \sum_{\mathbf{s}} H(\mathbf{s}), \tag{3.1}$$

$$H(\mathbf{s}) = \frac{g^2}{2a} \sum_{\mu} \mathcal{J}^2(\mathbf{s},\mu) - \frac{1}{g^2 a} \times \sum_{\mu>\nu} [\mathrm{Tr}(U_{\mathbf{s},\mu} U_{\mathbf{s}+\hat{\mu},\nu} U^{\dagger}_{\mathbf{s}+\hat{\nu},\mu} U^{\dagger}_{\mathbf{s},\nu}) + \mathrm{H.c.} - 6].$$

We use a lattice consisting of $L \times L \times L$ links, with periodic boundary conditions. (In our computer runs we will choose $L = 10$.) We label links by the pair $(\mathbf{s},\mu)$, where $\mathbf{s}$ is the site from which the link starts, with $0 \le s_x, s_y, s_z \le L \equiv 0$, and μ is the direction of the link. The DF on each link is an element of SU(3), represented by the fundamental representation matrix $U_{\mathbf{s},\mu}$ in the "magnetic" terms in Eq. (3.1). By $\mathcal{J}_{L,a}(\mathbf{s},\mu)$ we denote the generators of the gauge group, with $a = 1,\ldots,8$. The action of $\mathcal{J}_{L,a}$ on a matrix representation of SU(3) is to left multiply it by the ath generator matrix for that representation. $\mathcal{J}_{R,a}(\mathbf{s},\mu)$ acts to right multiply a representation in similar fashion, and $\mathcal{J}^2 = \sum \mathcal{J}^2_{L,a} = \sum \mathcal{J}^2_{R,a}$.

The Hamiltonian commutes with the generators of local gauge transformations at site $\mathbf{s}$:

$$\begin{aligned} Q_a(\mathbf{s}) = &-\mathcal{J}_{L,a}(\mathbf{s},x) - \mathcal{J}_{L,a}(\mathbf{s},y) - \mathcal{J}_{L,a}(\mathbf{s},z) \\ &+\mathcal{J}_{R,a}(\mathbf{s}-\hat{\mathbf{x}},x) + \mathcal{J}_{R,a}(\mathbf{s}-\hat{\mathbf{y}},y) \\ &+\mathcal{J}_{R,a}(\mathbf{s}-\hat{\mathbf{z}},z). \end{aligned} \tag{3.2}$$

Generators at different sites commute with each other, and generators at one site satisfy the Lie algebra of SU(3) generators. Physical eigenstates of the Hamiltonian are gauge invariant: They are eigenstates of all gauge generators with eigenvalue zero.

A. Gauge fixing

There are two ways to ensure that eigenstates are in this physical subspace of Hilbert space. One method is to change DF, with the new DF falling into two sets: "loop" variables and "maximal tree" variables [8, 9]. Then the general vector in the physical subspace is a general function of the loop variables, and does not depend upon the maximal tree variables. One can then construct a basis of functions of the loop DF, and be assured that the approximate eigenstates are physical. The difficulty with this approach is that the transformed Hamiltonian is no longer a sum of local terms $H(\mathbf{s})$, as in Eq. (3.1). Not only are terms highly nonlocal, they are no longer related by translation. However, all *practical* basis constructions we have been able to imagine rely on the locality and homogeneity of terms in the Hamiltonian. The crucial role played by these properties will become clear as we proceed. As a result, gauge fixing the Hamiltonian does not seem to be a useful choice for large lattices, even though it has been used in other situations [4, 6, 8].

B. Gauge-invariant basis states

A second way to ensure that approximate solutions of Schrödinger's equation are physical is to require that every state in the basis is gauge invariant. This has been done [2], but at the price of algebraic complexity. Furthermore, as we will argue below, the resulting basis is not well adapted to the computation of approximate eigenstates far from strong coupling. Perhaps a gauge-invariant basis can be put to practical use, but we have not chosen to pursue that goal in our work.

C. Extrapolation of colored states

The method we have chosen is to give up the quest for exact gauge invariance. Introduce the global color operator

$$Q^2 = \sum_{\mathbf{s}} \sum_{a=1}^{8} [Q_a(\mathbf{s})]^2 . \tag{3.3}$$

This operator commutes with H, and physical states have eigenvalue zero. Every other state has a positive expectation value. The spectrum of Q^2 is discrete, and eigenvalues are sums integer multiples of the quadratic Casimir eigenvalues of SU(3). The lowest nonzero eigenvalues are $4/3$, $8/3$,....

Consider the ground state of SU(3). Since the symmetry is unbroken we know the eigenvalue of Q^2 in the ground state: 0. When we use basis sets of the type described in Sec. II to construct upper bounds to the ground state energy, we find an expectation value q^2 that is positive. This is due to contamination of the basis with unphysical, colored states. By varying λ and t we obtain the dependence of the energy bound $\mathcal{E}_0(q^2)$ over a range that does not extend to zero. Our idea is to *extrapolate* the eigenvalue $\mathcal{E}_0(q^2)$ to $q^2 = 0$.

The justification for the crucial step of extrapolation is the following. If we had the exact eigenstates of H at our disposal, we could compute $\mathcal{E}_0(q^2)$ exactly, and it would fall on a curve in the $q^2 - E$ plane ending at the physical ground state at $q^2 = 0$. Because the energy we compute is a variational bound, our data will lie above the exact curve, but for intermediate values of q^2 we expect to parallel the exact curve. However, the curves we construct from our data will not generally extend to $q^2 = 0$. Instead, as we lower q^2 by increasing λ or t, $\mathcal{E}_0(q^2)$ must

finally begin to rise above the exact curve because states in the basis having very low q^2 are available at high energy, if they are present at all. We therefore will discard $\mathcal{E}_0(q^2)$ at its minimum and below, and extrapolation will be based on data obtained at intermediate values of q^2. The details are in Sec. VII.

There are practical tests of extrapolation. First, if the range of q^2 over which we have data is large compared to the range over which we extrapolate (long lever arm), and we discard data at small q^2 where $\mathcal{E}_0(q^2)$ begins to rise, extrapolation appears justified. The procedure is most apt to break down at weak coupling where many characters of SU(3) contribute to the harmonic oscillator single DF states. Fortunately, in just that limit we know all the answers from weak coupling perturbation theory, and can use them to check extrapolation.

There is an additional complication with excited states. When $q^2 \neq 0$, the first state above the ground state may be excited because the color content of the lattice has changed, not because a glueball is present. The remedy for this problem is to note that the colored states of the operator $\tilde{H} = H + rQ^2$, are lifted out of the low-energy spectrum when r is a positive number. In $\tilde{H}$ the energy of the colored states is artificially raised. Because both $\mathcal{J}^2(\mathbf{s},\mu)$ in Eq. (3.1) and $Q^2(\mathbf{s})$ in Eq. (3.2) are SU(3) Casimir operators, we expect the color term to be effective for $r \sim g^2/2$. We discuss this idea further in Sec. VII.

IV. THE STARTING STATE

At weak and strong coupling the properties of the ground state of pure SU(3) Hamiltonian lattice gauge theory are known. The energies and wave functions provide guides in selecting the starting state.

A. Weak coupling

At weak coupling it is useful to parametrize the elements of SU(3) as

$$U = \exp\left[ig\frac{\lambda\cdot\mathbf{r}}{2}\right]. \tag{4.1}$$

Then for small $\mathbf{r}$ the Hamiltonian density becomes quadratic:

$$H(\mathbf{s}) = \frac{1}{2a}\sum_{\mu}\nabla^2(\mathbf{s},\mu) + \frac{1}{2a}\sum_{\mu>\nu}[\mathbf{r}(\mathbf{s},\mu) + \mathbf{r}(\mathbf{s}+\hat{\mu},\nu) - \mathbf{r}(\mathbf{s}+\hat{\nu},\mu) - \mathbf{r}(\mathbf{s},\nu)]^2. \tag{4.2}$$

The ground state wave function in the physical $q^2 = 0$ subspace is Gaussian:

$$\psi_0 = \exp\left[-(1/g^2)\sum_{\{\mathbf{s}_i,\mu_i\}} M(\mathbf{s}_1,\mu_1;\mathbf{s}_2,\mu_2)\mathbf{r}(\mathbf{s}_1,\mu_1)\cdot\mathbf{r}(\mathbf{s}_2,\mu_2)\right], \tag{4.3}$$

where eigenvalues of M are of order 1. Note that the wave function is sharply peaked on SU(3), within distance $O(g)$ of the identity element of SU(3); this justifies the use of the small $\mathbf{r}$ Hamiltonian (4.3) at sufficiently weak coupling. The ground state energy in the color q^2 sector is

$$E_0(q^2) = 19.10L^3 + \frac{g^2q^2}{24}. \tag{4.4}$$

(In the weak-coupling limit the spectrum of Q^2 becomes continuous.)

When the coupling is not weak and must use the full SU(3) manifold, it is difficult to compute matrix elements of a nonseparable ground state, such as that of Eq. (4.3). We instead use a product of Gaussian-like factors on SU(3) for each degree of freedom. The weak coupling limit of the separable state we use is

$$\langle\{\mathbf{r}\}|0\rangle = \left[-(1/4t)\sum_{\mathbf{s},\mu}\mathbf{r}^2(\mathbf{s},\mu)\right], \tag{4.5}$$

where t is a variational parameter. When this trial state is used with Hamiltonian (4.3), the energy is minimized for $t = g^2/4$, and starting state results are

$$\mathcal{E}_0 = 24L^3, \quad \langle 0|Q^2|0\rangle = 48L^3/g^2. \tag{4.6}$$

We see that the starting state is colored. By Eq. (4.4) the bound $\mathcal{E}_0$ lies 14% above $E_0(q^2 = 48L^3/g^2)$, and 26% above $E_0(0)$.

B. Strong coupling

At $g = \infty$ the exact ground state is a constant independent of all DF. The ground state is a direct product of SU(3) singlets. In this limit the ground state energy $E_0(0)$ has dropped from $19.10L^3$ to zero. The first correction, given by the expectation of the Hamiltonian, is $18L^3/g^2$. It is useful to think of the constant wave function as the limit approached by a Gaussian whose width diverges. This suggests that a Gaussian of tunable width is a reasonable choice for each factor in the separable starting state, with the width being very narrow at weak coupling, and as broad as the SU(3) manifold at strong coupling. The width parameter is t.

C. The heat kernel

We can produce a tunable Gaussian wave function for a single DF on SU(3) by solving the heat equation on SU(3), which is [11]

$$\frac{\partial\phi}{\partial t} = -\mathcal{J}^2\phi. \tag{4.7}$$

The solution of this equation that is initially a δ function

on the group is

$$\phi(\{\alpha\},t)=\sum_{p,q=0}^{\infty} d(p,q)\chi^{(p,q)}(\{\alpha\})\exp[-t\lambda(p,q)], \tag{4.8}$$

where χ is the group character, $\{\alpha\}$ is a set of eight group parameters, d is the dimension of the p,q representation, and λ is the quadratic Casimir eigenvalue. The lattice starting state $|0\rangle$ is a separable product of single DF states

$$\langle\{\alpha\}|0\rangle=\prod_{\mathbf{s},\mu}\phi[\{\alpha\}(\mathbf{s},\mu),t]. \tag{4.9}$$

We find that when $g\sim 0.1$ or $t\sim 0.04$, more than 10^4 terms in (4.8) contribute to ϕ. This is because the group representations oscillate on the SU(3) manifold, and a superposition of many of them is required to produce a strongly peaked Gaussian. This observation indicates problems for bases such as that of Ref. [2], where gauge-invariance is ensured by coupling individual representations by Clebsch-Gordan coefficients. We do not see how to use a manageable set of such gauge-invariant basis functions to build up the strong peaking we know to be present at weak coupling. *We believe it is essential to build this Gaussian behavior into the weak coupling starting state* $|0\rangle$.

The operator $\mathcal{J}^2$ is simultaneously minus the Laplace-Beltrami operator and the quadratic Casimir operator. Therefore, the equation analogous to (4.7) on the flat weak-coupling manifold is obtained by putting $\mathcal{J}^2\to -\nabla^2$. Now we confirm Gaussian behavior and encounter the factors out of which we constructed trial wave function (4.5):

$$\phi\to\frac{\exp(-r^2/4t)}{(4\pi t)^4}. \tag{4.10}$$

The "diffusion time" t joins λ as a parameter labeling the basis states in our Krylov set.

Further "harmonic oscillator" states can be defined on SU(3), of which the first are ϕ_a and ϕ_{ab}. (The labels are SU(3) indices, $a,b=1,\ldots 8$.) Matrix elements of the operators of Kogut-Susskind Hamiltonian (3.1) between such states are available [3]. In this paper, lattice states will have each DF in either the Gaussian state ϕ or one of the octet of first excited harmonic oscillator states ϕ_a. We will not use the tensor.

V. LATTICE BASIS STATES

It is convenient to write each of the single DF operators in Hamiltonian (3.1) as the sum of an operator that is a multiple of the identity plus an operator whose expectation value in starting state (4.9) vanishes. When rewritten in terms of these operators, the effective Hamiltonian (2.6) becomes $\bar{H}\to\mathcal{E}_0+\bar{H}$, where the expectation value of the new $\bar{H}$ in starting state (4.9) vanishes. In the following, $\bar{H}$ denotes the new operator. Now when $\bar{H}$ is applied to $|0\rangle$, it necessarily produces a sum of states in which some of the DF on the lattice are excited.

The lattice states are

$$\psi_K=\sum_{i1,\ldots,iK}\bar{H}_{i1}\bar{H}_{i2}\cdots\bar{H}_{iK}|0\rangle, \tag{5.1}$$

where i's stands for a site label, and $\bar{H}_i=H(\mathbf{s})+\lambda\sum_a Q_a^2(\mathbf{s})$. Factors $\bar{H}_i$ and $\bar{H}_j$ that operate on at least one common DF are said to *communicate*. Factors that do not communicate commute, so we can rearrange terms in Eq. (5.1), setting off clusters of communicating factors by brackets:

$$\psi_K=\sum_{i1,\ldots,iK}\left[\bar{H}_{i\alpha}\bar{H}_{ib}\cdots\right]\left[\bar{H}_{i\alpha}\bar{H}_{i\beta}\cdots\right]\cdots|0\rangle. \tag{5.2}$$

When we sum over the i's, the same set of clusters appears $K!/(k1!k2!\cdots)$ times, where $k1,k2,\ldots$ are the numbers of Hamiltonian factors in clusters $1,2,\ldots$. Some of the clusters that we distinguish are actually equivalent, in the sense that they make the same contribution to ψ_K. Such clusters differ by commutation of neighboring Hamiltonian factors within the cluster that do not communicate with each other (although each communicates with some other factor in the cluster). We combine such equivalent clusters together, leading to additional counting factors $f1,f2,\ldots$ for clusters $1,2,\ldots$. We may rewrite Eq. (5.2) in the form

$$\psi_K=\sum_{\text{clusters}}\frac{K!f_1f_2\cdots}{k_1!k_2!\cdots}\left[\bar{H}_{i\alpha}\bar{H}_{ib}\cdots\right]\left[\bar{H}_{i\alpha}\bar{H}_{i\beta}\cdots\right]\cdots|0\rangle. \tag{5.3}$$

Our final manipulation is to rewrite the sum over clusters as a sum over cluster types and positions. This revision is possible because of the homogeneity of the Kogut-Susskind Hamiltonian (3.1). The replacement is

$$\sum_{\text{clusters}}=\sum_{\text{types}}\sum_{\text{positions}}\frac{1}{t_1!t_2!\cdots}, \tag{5.4}$$

where $t_1,t_2,\ldots$ are the numbers of clusters of types $1,2,\ldots$ on the lattice. These factors are required because when we sum over cluster positions independently, we overcount configurations that differ by the exchange of identical clusters. The factors $t!$ compensate for the overcounting. Altogether, we have the cluster decomposition of ψ_K:

$$\psi_K=\sum_{\text{types}}\sum_{\text{positions}}\frac{K!f_1f_2\cdots}{(k_1!k_2!\cdots)(t_1!t_2!\cdots)}\left[\bar{H}_{i\alpha}\bar{H}_{ib}\cdots\right]\times\left[\bar{H}_{i\alpha}\bar{H}_{i\beta}\cdots\right]\cdots|0\rangle. \tag{5.5}$$

We can use Eq. (5.5) to construct ψ_k if we know the amplitude factor and cluster pattern associated with each cluster. This observation motivates our computer code, which is designed to compute and store clusters.

A. Cluster approximations

We emphasize that it is permissible to make approximations that simplify the computation of the cluster amplitudes. The more accurately we compute the clusters,

the more accurate will be the eigenvalues and other matrix elements obtained from our approximate solutions of Schrödinger's equation. We can test the accuracy of our basis by making the basis larger, more faithful to Eq. (5.1), or more flexible, by means of variational parameters. λ and t can be regarded as variational parameters in this sense, and in this paper we have taken one further step to increase the flexibility of the basis. [See (E), below.] We approximate freely, motivated mostly by the desire to complete a reasonable first computation on a large lattice. Here is a list of our approximations.

(A) Each DF will be in harmonic oscillator state ϕ or ϕ_a. (Approximation 1.)

The starting state is invariant under simultaneous SU(3) transformation of all DF (even though it is not locally gauge invariant). As a result, when the Hamiltonian is applied repeatedly to the starting state, the resulting state is a global SU(3) singlet. There are many allowed couplings of color indices in such a state:

$$\mathrm{Tr}(\lambda_a\lambda_b)\phi_a\phi_b; \qquad \mathrm{Tr}(\lambda_a\lambda_b\lambda_c)\phi_a\phi_b\phi_c; \quad \ldots . \tag{5.6}$$

On the cube, the dominant states are those coupled with the first of these couplings, where pairs of color indices are contracted [5]. We retain only those excited states with pairwise index contractions (Approximation 2).

Altogether, our excited states consist of a single pair of excited states, with color indices contracted. In the following we refer to such states as pairs. Because of the homogeneity of the Hamiltonian, pair states that differ by translation are equivalent. Taking this into account, there are $(9L^3+6)/2$ pair states on the lattice when L is even, and $(9L^3+9L^2-12)/2$ pair states when L is odd.

(B) Pair states are indexed by the integer k designating how many times $\bar{H}$ has been applied to the starting state in producing the pair. The first time $\bar{H}$ acts on $|0\rangle$ it produces a pair whose links share a plaquette or site. Using Eq. (2.4) we obtain the amplitude for each of these pairs, and all other pairs have amplitude zero. When $k > 1$, pairs consisting of more widely separated links begin to have nonzero amplitudes. The relative magnitudes and signs of these amplitudes depend on g, λ, and k, and are determined dynamically. The amplitudes are stored as $A_k(j)$, where j designates the pair type.

(C) Each time $\bar{H}$ is applied to a pair, the pair can be left unchanged, one or both links forming the pair can move, or the pair can be annihilated. Annihilation can occur when the links of the initial pair share a plaquette or site. As we apply $\bar{H}$ repeatedly to generate pairs of higher k, we retain only *new* pairs. This means each pair contributes only to one application order k. (Approximation 3.) We also ignore pair annihilation. However, this is not an additional approximation because further applications of $\bar{H}$ merely reproduce pair amplitudes already present.

(D) According to Eq. (5.5), all DF that are excited at any time in the course of producing a pair are included in a cluster; that is, a cluster consists of a pair plus the surrounding DF that were excited and have returned to state ϕ. This leads to a large number of clusters that contain the same excited pair, but differ in the specification of the surrounding DF included in the cluster. In principle, the distinction must be retained because if two clusters "overlap" so that they share any DF, they merge into a single pair. Much bookkeeping is required to follow such distinguished clusters, and we choose to combine the amplitudes of clusters containing the same pair without regard to which surrounding DF are excited as $\bar{H}$ is applied repeatedly. In Eq. (5.5), we take two clusters to be nonoverlapping if they share no common excited links. (Approximation 4.)

(E) In state ψ_K, $\sum_i k_i = K$, so that the set $\{k_i\}$ is a partition of K. Accordingly, there are contributions to ψ_K differing in the number of nonzero k's and hence in the number of pairs on the lattice. Following a suggestion in Ref. [1], we separate these contributions, and retain each as an individual state in our basis. Thus, our basis states are labeled by K and a second integer N, $N = 1, \ldots K$, which designates the number of pairs. In the following we write $K = N + n$, with $n = 0, 1, \ldots$. The state $\psi_{N,n}$ is the sum of those terms in Eq. (5.5) in which $K = N+n$ has been partitioned into N positive integers. This is a step that broadens the flexibility of the basis.

(F) In Sec. I we pointed out that it is desirable to retain states in which all DF are excited, so we take basis states in which $N = 1, \ldots, 3L^3/2$, which is 1500 on our $10 \times 10 \times 10$ lattice.

It is also desirable to include pairs with widely separated links. Let us designate the maximum number of $\bar{H}$'s acting in a given pair state by $k_{\max}$. We also impose the limit $n_{\max} = k_{\max} - 1$. In this paper we have taken $k_{\max} = 6$. (Approximation 6.) Most pairs on the lattice are therefore produced by one application of $\bar{H}$, but a few have been produced with more applications: one pair on the lattice may have $k = 6$; two pairs may have (2,5) or (3,4); three pairs may have (2,2,4) or (2,3,3); four pairs may have (2,2,2,3), and five pairs may have $k = 2$. In each case, the limitation on widely separated pairs is undoubtedly the worst defect in our basis because one can expect scaling to emerge only when many DF are correlated with distant DF. Increasing $k_{\max}$ in future work has high priority, and we have ideas about how to do that in a tractable basis.

VI. MATRIX ELEMENTS

The lattice states we have set up are not orthonormal, so the eigenvalue equation we must solve takes the form

$$\sum_{P,p} \tilde{H}(N,n;P,p)V(P,p) = \mathcal{E}\sum_{P,p} M(N,n;P,p)V(P,p), \tag{6.1}$$

where $V(P,p)$ is an eigenvector, $\mathcal{E}$ is the eigenvalue (to which must be added the displacement $\mathcal{E}_0$), and M is the metric matrix

$$M(N,n;N',n') = \langle \psi_{N,n} | \psi_{N',n'} \rangle. \tag{6.2}$$

We first consider the computation of M. The reader should recall at this point that approximations were

made freely in setting up $\psi_{N,n}$; the worst an approximation can do is diminish the effectiveness of the basis. By constrast, approximations made in the evaluation of the matrices H and Q must be justified.

When we use Eq. (5.5) to evaluate M, there is a nonzero contribution only when the same links are excited in the bra and ket states. Hence, the only nonzero matrix elements are $M(N,n;N,n')$ with $0 \leq n,n' \leq k_{\max}-1$. Contributions to this matrix element come from terms in the bra and ket states having identical patterns of unexcited and excited link DF. It is not necessary that the excited links in bra and ket be grouped into identical pair states, but it is the case that contributions where they are so grouped dominate those where they are not. Later we will show that domination is by powers of the lattice volume L^3, which in our case is 10^3. We retain only those contributions where the pairs in the bra and ket are identical, ignoring the $O(1/L^3)$ correction. In this approximation the matrix $M(N,n;N,n')$ is zero when $n \neq n'$, for then some of the pairs in bra and ket must differ. The states are now orthogonal, and $M(N,n;N,n)$ is the norm of the state.

Consider the contribution of a particular configuration of N pairs to $M(N,n;N,n')$. The contribution is independent of the positions of these pairs on the lattice, and the sum over positions [in Eq. (5.5)] leads to a multiplicative counting factor ρ. ρ counts the number of ways the N pairs can be placed on the lattice without overlap. The requirement of "no overlap" causes the computation of ρ to depend on the particular set of pairs under consideration. It is evidently complicated to compute ρ precisely. However, things are simple when we ask for ρ for N *randomly* chosen pairs.

Suppose that N pairs have been placed on the lattice, which can be done in $\rho(N)$ ways. Now consider the addition of the randomly chosen $(N+1)$st pair. There are L^3 links on which we can try to place the first link of the new pair, and the probability that the link we choose is not excited is $(3L^3-2N)/(3L^3)$. Given that the position for the first link is available, the probability that the second link lands on an unexcited link is $(3L^3-2N-1)/(3L^3-1)$. Altogether, the expected number of positions for the new pair is

$$\frac{\rho(N+1)}{\rho(N)} = L^3\left[1-\frac{2N}{3L^3}\right]\left[1-\frac{2N}{3L^3-1}\right]. \tag{6.3}$$

The solution of this recursion relation with boundary condition $\rho(1)=L^3$ is

$$\rho(N) = \left[\frac{1}{9L^3-3}\right]^N \frac{\Gamma(3L^3+1)}{\Gamma(3L^3+1-2N)}. \tag{6.4}$$

It should be pointed out that when we compute the matrix elements of the operators H and Q^2, we encounter ratios like $\rho(N+a)/\rho(N)$, with $a=1,2$. These ratios are very close to $(L^3)^a$. [See Eq. (6.3.)] Because the corrections have relative magnitude $O(1/L^3)$ for any set of N pairs, the statistical evaluation is adequate.

We can now show that contributions to M having identically paired excited DF in the bra and ket dominate contributions where the excited DF are differently paired in the bra and ket. We again use statistical reasoning. Start with N (identical) pairs on the lattice, and add four more excited links. When these four links are organized into identical pairs, the counting factor is $\rho(N+2)$. When the pairs in bra and ket are different, the counting factor (designated $\rho'(N+2)$) is

$$\frac{\rho'(N+2)}{\rho(N)} = \frac{2L^3}{8}\left[1-\frac{2N}{3L^3}\right]\left[1-\frac{2N}{3L^3-1}\right] \times\left[1-\frac{2N}{3L^3-2}\right]\left[1-\frac{2N}{3L^3-3}\right]. \tag{6.5}$$

The factor 2 is present because there are two ways to form distinct pairs using the four added links in the bra and ket states; 1/8 arises from a color sum: When the pairs in bra and ket are identical there are two color sums, but when they are different there is only one. Comparison of the two counting factors shows the dominance of the case where the pairs in bra and ket are identical:

$$\frac{\rho'(N+2)}{\rho(N+2)} = \frac{3(3L^3-1)}{4(3L^3-2)(3L^3-3)} \sim \frac{1}{4L^3}. \tag{6.6}$$

This line of reasoning can be applied to larger groups of excited states, with the conclusion that the dominant contributions always arise when the excited states in bra and ket are identical.

After summation over position, the matrix element $M(N,n;N,n')$ can be expressed in the form

$$M(N,n;N,n') = \rho(N)\frac{\partial^{N+n}}{\partial x^{N+n}}\frac{\partial^{N+n'}}{\partial y^{N+n'}}G_N(x,y)\Big|_{x=y=0}, \tag{6.7}$$

where the generating function is obtained from the pair amplitudes

$$G_N(x,y) = \frac{1}{N!}\left\{\sum_{j=1}^{j_0}\left[\sum_{k=1}^{k_{\max}}\frac{A_k(j)x^k}{k!}\right] \times\left[\sum_{\bar{k}=1}^{k_{\max}}\frac{A_{\bar{k}}(j)y^{\bar{k}}}{\bar{k}!}\right]\right\}^N. \tag{6.8}$$

j_0 is the index of the "last" pair type. The correctness of Eq. (6.7) is verified by using the multinomial theorem (twice) to evaluate the partial derivatives. The result is

$$M(N,n;N,n') = (N+n)!(N+n')!\rho(N)\prod_{j=1}^{j_0}\prod_{k=1}^{k_{\max}}\sum_{s(1,j),\ldots,s(k_{\max},j)}\sum_{\bar{s}(1,j),\ldots,\bar{s}(k_{\max},j)}\frac{s_j!}{s(k,j)!\bar{s}(k,j)!} \times\left[\frac{A_k(j)}{k!}\right]^{s(k,j)}\left[\frac{A_k(j)}{k!}\right]^{\bar{s}(k,j)}, \tag{6.9}$$

where the indices are non-negative integers constrained by the conditions

$$N=\sum_{j=1}^{j_0} s_j,$$
$$s_j=\sum_{k=1}^{k_{\max}} s(k,j)=\sum_{k=1}^{k_{\max}} \bar{s}(k,j), \tag{6.10}$$
$$N+n=\sum_{k=1}^{k_{\max}}\sum_{j=1}^{j_0} k s(k,j),$$
$$N+n'=\sum_{k=1}^{k_{\max}}\sum_{j=1}^{j_0} k \bar{s}(k,j).$$

The factor $s_j!$ in Eq. (6.9) counts the number of ways the s_j identical pairs of type j can be matched in bra and ket. The factors $[k!]^{s(k,j)}$ are the $k_1!k_2!\ldots$, and the factors $s(k,j)!$ are the $t_1!t_2!\cdots$ in Eq. (5.5). In our basis, amplitudes $A_k(j)$ are nonzero only when k and j are related. The reader may verify that under these circumstances, the constraints in Eq. (6.10) can be satisfied only when $n=n'$.

Equation (6.9) exhibits the danger that M may be noncomputable. Even for quite modest $k_{\max}$, j_0 can be several thousand. Then if constraints (6.10) allow each $s(k,j)$ to take even two values, the sums indicated in Eq. (6.9) run over 2^{2j_0} terms, and they cannot be carried out. However, the expression for the generating function can be rearranged so that the sum over j is carried out before sums over the k's occur. This rearrangement makes M easy to compute. Introduce the matrix

$$C_{k,\bar{k}}=\sum_{j=1}^{j_0}\frac{A_k(j)A_{\bar{k}}(j)}{k!\bar{k}!}. \tag{6.11}$$

Then use of the multinomial theorem leads to the rearranged formula

$$M(N,n;N,n')=(N+n)!(N+n')!\rho(N)\times\sum_{\{t(k,\bar{k})\}}\prod_{k,\bar{k}=1}^{n_{\max}}\frac{(C_{k,\bar{k}})^{t(k,\bar{k})}}{t(k,\bar{k})!}. \tag{6.12}$$

In this equation we maintain the constraints

$$N=\sum_{k,\bar{k}=1}^{k_{\max}} t(k,\bar{k}),\qquad N+n=\sum_{k,\bar{k}=1}^{k_{\max}} k t(k,\bar{k}),$$
$$N+n'=\sum_{k,\bar{k}=1}^{k_{\max}} \bar{k} t(k,\bar{k}). \tag{6.13}$$

The number of non-negative integer partitions of N subject to these constraints is independent of N and manageably small. For example, for $n,n'=3,4$ there are 13 sets of $t(k,\bar{k})$. For 6,6 and 8,8, the number of partitions is 1043 and 8406, respectively.

The computations of the matrices H and Q^2 parallel that of M. Factors ρ arising sums over pair positions are evaluated statistically. Again there are generating functions that provide the correct combinatorial factors, and again these generating functions can be rearranged so that the sum over pair types is done first. A new feature is that in $H(N,n;N',n')$, N and N' can differ by as much as two; in $Q^2(N,n;N',n')$ they can differ by one. We omit the details of the calculation of these additional matrices. It is important to note that these matrices are sparse, each having about 10^5 nonzero elements. We therefore compute the matrix elements just once and store them.

We compute the eigenstates of $\tilde{H}$ by constructing the Krylov states in the 9001 dimensional vector space. A few hundred Krylov states suffice to compute eigenvalues to double precision accuracy. In this process the sparseness of H and Q^2 are a major help because adding a new state involves $\sim 10^4$ operations, not $\sim 10^8$.

VII. NUMERICAL RESULTS

An estimate for the ground state energy is obtained by adding $\mathcal{E}_0$ to the lowest eigenvalue produced by Eq. (6.1). This energy and the expectation of the color operator Q^2 both depend on the parameters λ and t that fix the basis. In Fig. 1 we illustrate how these energies vary when λ is varied for fixed $t=0.0095$ and $g=0.2$ (a weak coupling). This value of t corresponds to single DF wave functions that are peaked near the identity of SU(3); the peaking is achieved by superposing about 5000 characters of the group. The abscissa of Fig. 1 is the color density multiplied by g^2: color$=g^2\langle Q^2\rangle/L^3$, and the ordinate is the ground state energy density. It is to be expected that the bases for very negative and very positive λ are the same because then $\tilde{H}$ is dominated by the color operator, and changing the phase of the basis states has no effect.

When t is changed, a sequence of curves similar to that

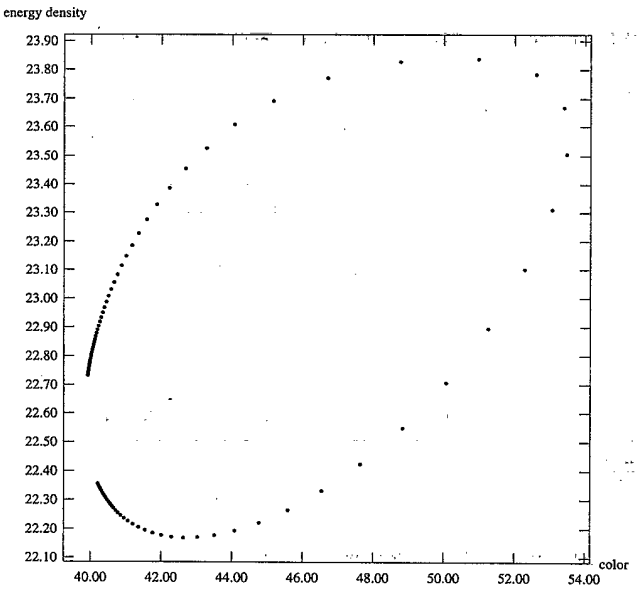

FIG. 1. Ground state energy density vs scaled color density at $g=0.2$, $t=0.0095$. Basis parameter λ varies from -0.06 to $+0.03$ in steps $\Delta\lambda=0.001$. Data points traverse plot in clockwise sense as λ increases.

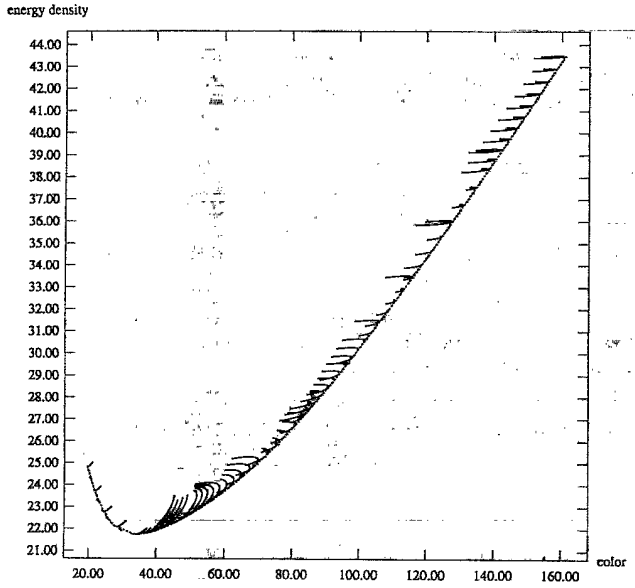

FIG. 2. Data at $g = 0.2$ for 111 different values of t (solid curves). Dashed curve is bounding envelope of best ground state energy vs *color*.

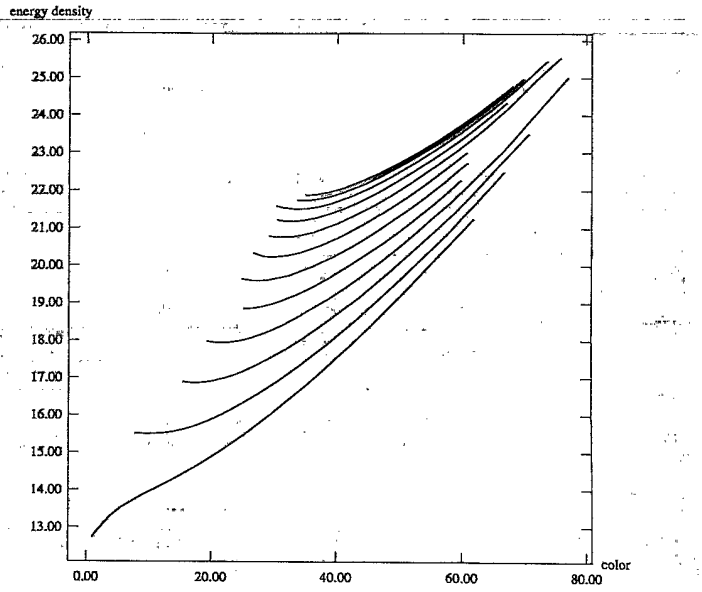

FIG. 3. Envelope curves for $g = 0.1$ (top) in steps $\Delta g = 0.1$ to $g = 1.2$ (bottom).

in Fig. 1 is obtained. In Fig. 2 we show a number of these curves at $g = 0.2$, together with the envelope curve bounding them from below; this envelope is the plot of energy density vs *color* that is given by our calculation. We see that the basis is deficient in states of very low *color*, because when we increase t to reduce *color*, low-energy states can no longer be formed, and the envelope curve rises. It is easy to see that this must happen at weak coupling because to reach *color* $= 0$ we must take $t \to \infty$. In this limit the single DF wave functions become flat on SU(3), and the starting state approaches a direct product of SU(3) singlet states. (This starting state is locally gauge invariant, which is why *color* $= 0$.) But then we can take the expectation value of Eq. (3.1) in the starting state to obtain an analytic expression for the energy density at *color* $= 0$: $18/g^2$. (This is the first nonzero term in Hamiltonian strong-coupling perturbation theory.) In Fig. 2, this limiting energy density is huge: 450. We discard the parts of the envelope curves lying to the left of the minimum energy.

Figure 3 shows the envelope curves for twelve values of g separated by intervals $\Delta g = 0.1$. At the top $g = 0.1$, and at the bottom $g = 1.2$. The left ends of the envelope curves are located at approximately the point where the energy is a minimum. We see that as g increases, the envelopes extend to smaller values of *color* before rising.

The bottom envelope curve in Fig. 3 has $g = 1.2$. It appears to be approaching a minimum at the physical limit of *color* $= 0$. The leftmost point on this curve corresponds to $t = 2$, which means that the starting state is predominantly SU(3) singlet. A linear extrapolation from the left end of the curve to *color* $= 0$ gives a physical energy density of about 12.5, which is $18/g^2$. This suggests that for $g > 1.2$ we can extrapolate to *color* $= 0$ but the extrapolant is the first nontrivial term in strong-coupling perturbation theory. In future we hope to extend the basis state set, and then we expect the extrapolation to the strong-coupling expression will occur at higher values of the coupling.

The curvature of the remaining envelopes in Fig. 3 makes it difficult to extrapolate them to *color* $= 0$. However, when we compare envelope curves for g and $g + 0.1$, the curvatures are similar, and the difference in ground state energy densities has a much more linear dependence on *color*. In Fig. 4 we plot the difference in the ground state energy densities at $g = 0.4$ and $g = 0.5$. In order to produce Fig. 4 we have had "subtract" envelope

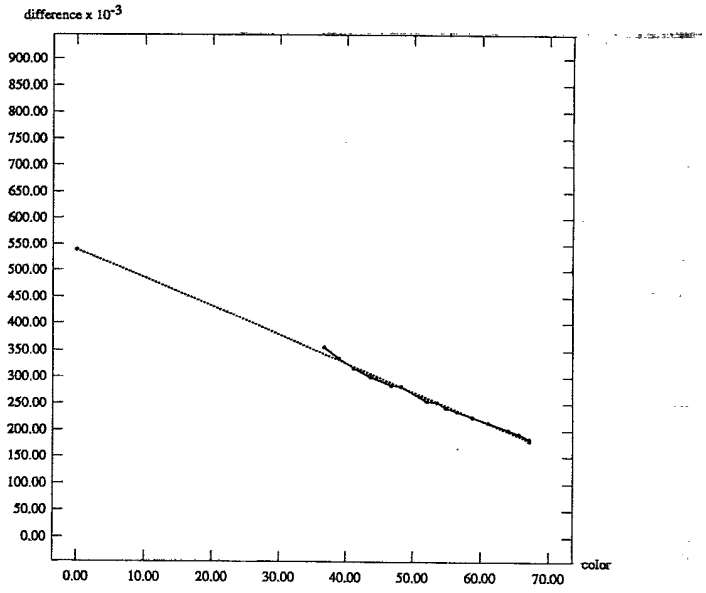

FIG. 4. Difference between ground states energy densities at $g = 0.4$ and $g = 0.5$ vs *color*. The dashed line gives the linear extrapolation to the physical limit.

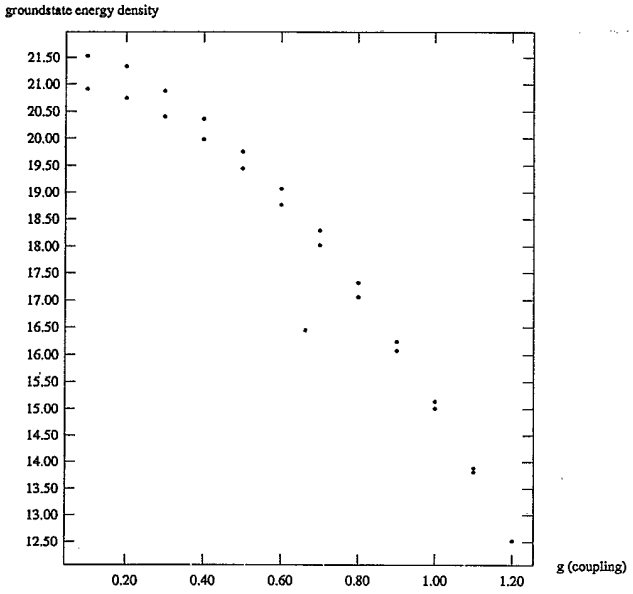

FIG. 5. Ground state energy density at the physical limit vs g. Data obtained by adding energy difference at each g.

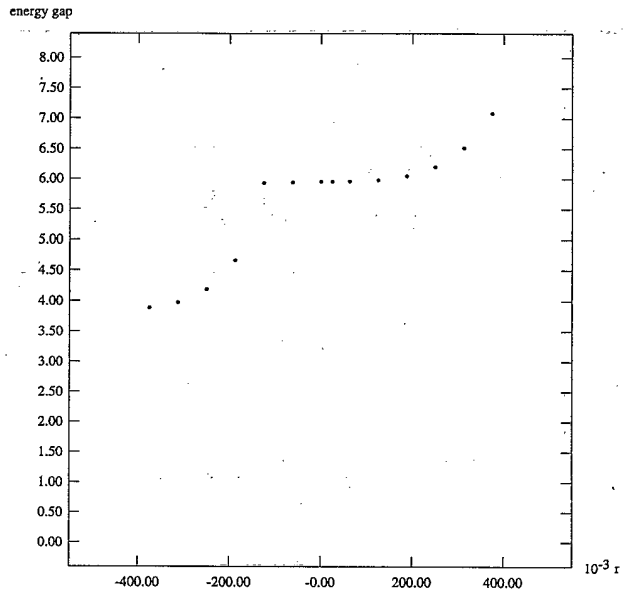

FIG. 6. Energy gap vs parameter r. The plateau near $r = 125 \times 10^{-3}$ allows gap measurement to be made.

curves generated from data taken at different values of *color*. Therefore, the subtraction requires interpolation on one of the envelopes, and we find some sensitivity to the method of interpolation. This uncertainty could be eliminated by taking data on all curves at the same *color* values—a laborious task.

The crucial assumption in the extrapolation to *color* = 0 is that linear behavior is maintained over the extrapolation interval. Looking at Fig. 4, linear extrapolation is plausible, and as we will see below, the procedure satisfies an important consistency check. When we extend the basis state set we expect to be able to extend the curves of Fig. 4 to smaller *color* and reduce the interval of extrapolation. If the data in the extended interval remains linear, the assumption of linear extrapolation will be supported.

In Fig. 5 we give the ground state energy density as a function of coupling. Weak-coupling perturbation theory gives the exact density at zero coupling: 19.1 [Eq. (4.4)]. The upper (lower) data points are generated by taking the larger (smaller) estimates of ground state energy difference (at *color* = 0) at each g. Our weak coupling energy density at $g = 0.1$ lies about 10% above the exact result at $g = 0$.

The ability to compute the physical ground state energy density throughout the interval from strong coupling to (essentially) zero coupling is an important benchmark for our program. It tests the idea of *color* extrapolation. However, the ground state energy is cutoff dependent and unphysical; it is the energy gaps that have potential physical significance as glueballs. Realistic gaps must await further work because we have included few long-distance pairs in the bases. Our energy gaps will therefore be determined by our correlation length of essentially one lattice spacing, and not (at weak coupling) by the size of the lattice. However, there are still useful checks to be made. Recall that we proposed computing eigenstates of the operator $\tilde{H} = H + rQ^2$ because this operator, unlike H, has no low-lying colored states in its spectrum for $r > 0$. Comparison with the normal electric operator suggested that r should be set $\sim g^2/2$. However, this idea introduces a new parameter, r, and we can make useful gap predictions only if the energy gap is independent of r for $r \sim g^2/2$. In Fig. 6 we show data taken at $g = 0.5$ and *color* = 40. There is a very level plateau near $r = 0.125 = g^2/2$, which is required for our strategy to work. Note that when we take $r < 0$ the gap changes. We believe this is caused by the presence of colored states

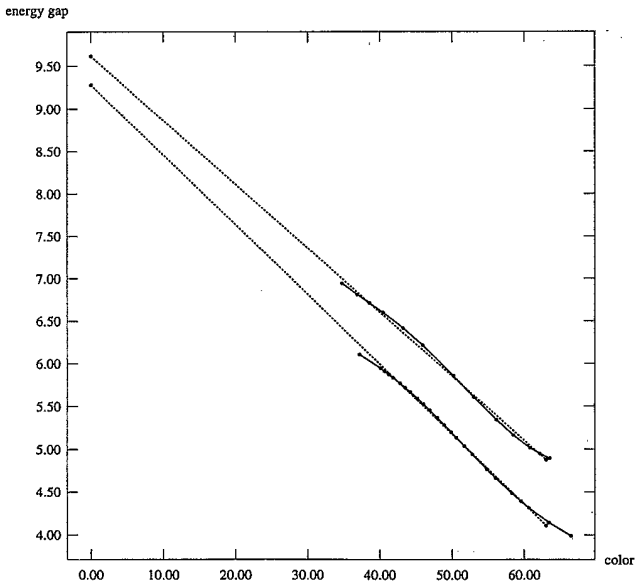

FIG. 7. Energy gap vs *color* at $g = 0.1$ (top) and $g = 0.5$ (bottom). Dashed lines are linear extrapolations to the physical limit.

in the low-energy spectrum of $\tilde{H}$ when $r < 0$.

The *color* plotted in Fig. 7 requires explanations. Denote the two lowest-lying eigenstates of $\tilde{H}$ by ψ_0 and ψ_1 and define the matrix elements $E_{ij} = \langle\psi_i|H|\psi_j\rangle$, and $Q^2_{ij} = \langle\psi_i|Q^2|\psi_j\rangle$. We have tuned t and λ to minimize E_{00} at specified Q_{00}. We point out that Q_{00} and Q_{11} are similar, but they are not identical, so we define *color* in terms of their average: $color = g^2(Q^2_{11} + Q^2_{00})/(2L^3)$. This definition has an advantage. When we extrapolate to $color = 0$, we necessarily reach $Q^2_{00} = 0$ *and* $Q^2_{11} = 0$ because Q^2 is a positive operator.

We define the energy gap to be $E_{11} - E_{00}$. Note that although eigenstates ψ_0 and ψ_1 are not connected by $\tilde{H}$, in general they are connected by H: $E_{01} = -rQ^2_{01} \neq 0$. However, when we extrapolate to $color = 0$, the conditions $Q^2_{00} = Q^2_{11} = 0$ imply $Q^2_{01} = 0$ as well, and in the physical limit, the energy gap (as we have defined it) extrapolates to the difference between the energies of the two lowest eigenstates of H.

In Fig. 7 we show the energy gap as a function of *color* at $g = 0.1$ and $g = 0.5$. The curves show that the energy gaps depend linearly on *color*, allowing linear extrapolation to the physical limit $color = 0$. The ability to make a convincing extrapolation of the energy gap is a second check on the viability of our approach.

In Fig. 7 the energy gap corresponds to a correlation length of about one lattice spacing, and is essentially independent of coupling. These results are unphysical, but they are to be expected with our basis, which has very few long-range pairs. We see that our basis must be improved by adding many long-range pairs. We hope to report results based on such an improved basis in a moderate period of time.

ACKNOWLEDGMENTS

This work was supported in part by the National Science Foundation under Grant No. PHY 91-21039.

[1] A. Duncan and R. Roskies, Phys. Rev. D **31**, 364 (1985).
[2] J. Piekarewicz, M. R. Zirnbauer, and S. E. Koonin, Int. J. Mod. Phys. A **3**, 409 (1988).
[3] J. B. Bronzan and T. E. Vaughan, Phys. Rev. D **44**, 3264 (1991).
[4] J. B. Bronzan and T. E. Vaughan, Phys. Rev. D **43**, 3499 (1991).
[5] Yuksel Gunal (unpublished).
[6] T. E. Vaughan, Ph.D. thesis, Rutgers University, 1992 (unpublished).
[7] J. B. Kogut and L. Susskind, Phys. Rev. D **11**, 395 (1975).
[8] V. F. Müller and W. Rühl, Nucl. Phys. **B230**, 49 (1984).
[9] J. B. Bronzan, Phys. Rev. D **31**, 2020 (1985).
[10] E. C. Kemble, *The Fundamental Principles of Quantum Mechanics* (McGraw-Hill, New York, 1937), pp. 408–416.
[11] J. B. Bronzan, Phys. Rev. D **40**, 3494 (1989).